Journal of Materials Chemistry B

PAPER

Improved polyvinylpyrrolidone microneedle arrays with non-stoichiometric cyclodextrin

Cite this: *J. Mater. Chem. B*, 2014, **2**, 1699

Wei Chen,[ab] Chong Wang,[ab] Li Yan,[ab] Longbiao Huang,[ab] Xiaoyue Zhu,[ab] Bing Chen,[c] Himanshu J. Sant,[d] Xinrui Niu,[c] Guangyu Zhu,[e] K. N. Yu,[b] V. A. L. Roy,[ab] Bruce K. Gale[d] and Xianfeng Chen*[ab]

Received 30th November 2013
Accepted 7th January 2014

DOI: 10.1039/c3tb21698e

www.rsc.org/MaterialsB

Dissolving polymer microneedles have attracted much attention for their biocompatibility, fast dissolution, and high drug loading. Among them, polyvinylpyrrolidone (PVP) is widely used, but its high water absorption and poor mechanical properties constrain its broad applications. Herein we show that adding cyclodextrin (CD) to form PVP–CD inclusion complexes can alleviate these problems. The water absorption of PVP was reduced by 36–40% at different RHs as the PVP–CD inclusion complexes formed. Attractively, the water absorption at 10 and 20 days remained almost the same for the complexes while it could dramatically increase for the pure PVP samples, particularly in high humidity environments, indicating a possibly longer storage time for the complexes. It was also found that the Young's modulus and hardness of the PVP–CD could be greatly improved, especially for low molecular weight PVP. Furthermore, the glass transition temperature (T_g) of the PVP–CD increased by up to 39 °C. With the improved properties, the fabricated PVP–CD microneedles possessed much sharper needle tips and the patch had less cracks than those made from pure PVP. Pig skin application results suggested that the PVP–CD microneedle arrays were able to reliably pierce the stratum corneum of the skin while it was not achievable for the PVP microneedles with the same geometry. We anticipate that these PVP–CD complex microneedles are more suitable for vaccine and drug delivery because of their superior properties.

Introduction

Microneedle patches are arrays of ultra-small needles with lengths well below one millimetre[1,2] and are broadly used for transdermal delivery of vaccines and drugs. Their major advantages include the ability to pierce skin in a non-invasive way and they can be integrated into "lab-on-a-chip" systems for monitoring glucose levels, *etc.*[3] These microneedles are often made of metals,[4,5] silicon,[6,7] and polymers.[8–10] Among them, dissolving polymer microneedles attract great attention for their biocompatibility, biodegradability, low price, and high drug or vaccine loading. Polymers such as chitosan,[11] polyacrylic acid (PAA),[9] carboxymethyl cellulose (CMC),[12] polyvinylpyrrolidone (PVP),[13] silk,[14] and sugar glass[15] have been reported for preparing dissolving microneedles. However, compared to metal and silicon microneedle arrays, dissolving ones usually have two disadvantages. One is their low mechanical strength hindering consistent and reliable penetration into the skin.[3] The other is hygroscopicity, which is particularly serious for polymers like PVP. PVP shows excellent biocompatibility and water solubility and therefore is often used as a main component for temporary skin covers and wound dressing.[16] PVP is also used in the pharmaceutical industry as a coating agent, polymeric membrane, and material for controlled drug release.[17] Although PVP has been reported to make microneedles, its poor mechanical properties and strong water absorption seriously limit the practical usage, especially for low molecular weight PVP.

Cyclodextrin (CD), manufactured from starch, has been widely used in the pharmaceutical industry for drug coating and delivery.[18] β-CD is the most accessible and the lowest-priced type. During oral administration, it is minimally irritating and has many advantages including very small amounts (1–2%) being absorbed in the upper intestinal tract, no metabolism happening in the upper intestinal tract, and being able to be metabolized by bacteria in the caecum and colon.[19] It is known that CD can form inclusion complexes (host–guest complexes) with a very wide range of solid, liquid and gaseous compounds

[a]*Center of Super-Diamond and Advanced Films (COSDAF), City University of Hong Kong, Hong Kong SAR, P. R. China*

[b]*Department of Physics and Materials Science, City University of Hong Kong, Hong Kong SAR, P. R. China. E-mail: xianfeng.chen@cityu.edu.hk; Fax: +86 3442 0538; Tel: +86 3442 7813*

[c]*Department of Mechanical and Biomedical Engineering, City University of Hong Kong, Hong Kong SAR, P. R. China*

[d]*State of Utah Center of Excellence for Biomedical Microfluidics, Departments of Bioengineering and Mechanical Engineering, University of Utah, Salt Lake City, UT 84112, USA*

[e]*Department of Biology and Chemistry, City University of Hong Kong, Hong Kong SAR, P. R. China*

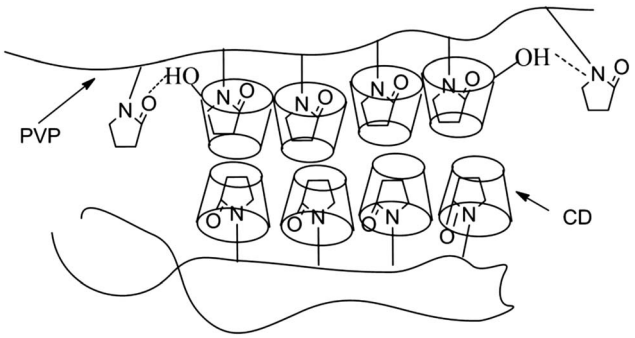

Fig. 1 Schematic diagram of PVP–CD complexes.

by molecular complexation. The hydrophobic cavity of CD molecules provides a microenvironment for appropriately sized non-polar moieties to enter and form inclusion complexes, with no covalent bonding between CD and moieties.[20–23] Replacement of water in the cavity by hydrophobic guest molecules leads to reduction of enthalpy, which is the main driving force of formation of these host–guest complexes.[24] The complexes can be formed in either solution or solid state. Being locked or caged within the CD cavity gives rise to beneficial modifications of the guest molecules including enhanced solubility,[25,26] anti-oxidation under visible or UV light or heat, controllability of volatility and sublimation, physical isolation of incompatible compounds, masking off unpleasant odors[27] and controlled drug release.[28]

Making use of the advantages of such host–guest complexes, we hypothesize that the formation of PVP–CD inclusion complexes can greatly decrease the water absorption of PVP (Fig. 1). In the meantime, the hydroxyl group of the outer cavity of CD can form hydrogen bonding with PVP, which will restrict the movement of the PVP chain and correspondingly increase the mechanical strength.

To validate the hypothesis, in our work, we investigated the effect of adding two types of CD (hydroxypropyl-β-cyclodextrin (HP-β-CD) and dimethyl-β-cyclodextrin (DIME-β-CD)) into PVP of two different molecular weights (M_n = 58 000 (named as PVP58) and M_n = 10 000 (named as PVP10)).

Experimental section

Materials

PVP58, PVP10, sodium chloride, potassium chloride, potassium acetate, HP-β-CD and DIME-β-CD were purchased from Sigma Aldrich. Poly(dimethylsiloxane) (PDMS, SYLGALD® 184) was ordered from Dow-Corning. All of the materials were used without further treatment.

Inclusion complex preparation

The non-stoichiometric PVP58 and HP-β-CD inclusion complexes were prepared according to the following procedures. Briefly, 50 mg of PVP58 and 50 mg of HP-β-CD were dissolved in 1 ml of water followed by 30 minutes of sonication and 1 day of stirring. Secondly, the composite was placed at room temperature for two days until the water evaporated. After that, the sample was placed into containers containing various saturated salt solutions for relative humidity (RH) control. The product was named as PVP58–HP-β-CD-11 ("11" indicates that the weight ratio of PVP to HP-β-CD was 1 : 1). Other samples including PVP58–HP-β-CD-51, PVP10–HP-β-CD-11, PVP10–HP-β-CD-51, PVP58-DIME-β-CD-11, PVP58-DIME-β-CD-51, PVP10–DIME-β-CD-11, and PVP10–DIME-β-CD-51 were prepared using the same process. PVP58 and PVP10 films were prepared using a similar process without adding CD.

Microneedle array preparation

The complex microneedle arrays were prepared according to the previously reported methods.[8,29] A mould was prepared by applying a PDMS base and crosslinking agent with a volume ratio of 10 : 1 to a silicon master microneedle array followed by curing at room temperature for two days. To make polymer microneedles, PVP or PVP–CD aqueous solution was cast onto the PDMS mould. The solution was forced into the microneedle cavity in the mould by a vacuum environment. After drying at room temperature for two days, high concentration PVP58 or PVP10 solution (50 wt%) was cast to form the base of the microneedle patch.

Water absorption under various relative humidity conditions

PVP–CD complexes were first placed in a dry desiccator for two days to allow all samples to have equivalent conditions before water absorption measurement. Then the samples were stored at ambient temperature under various controlled RH conditions by using saturated salt solutions of potassium acetate (23% RH), sodium chloride (75% RH), and potassium chloride (85% RH).[30] Subsequently, water absorption was determined using a gravimetric method by drying samples in a vacuum oven at an elevated temperature of 50 °C until a constant weight was achieved. The water content was calculated as the weight loss after drying in relation to the weight of the sample before temperature elevation.

Differential scanning calorimetry (DSC)

The glass transition temperatures (T_g) of samples were tested by DSC (TA Q1000) under a nitrogen atmosphere. The first cycles were performed from 50 °C to 230 °C at a temperature increase rate of 10 °C min^{-1} and then maintained at 230 °C for 3 min to erase any previous thermal history. After that, the samples were cooled down to 50 °C at a rate of 30 °C min^{-1}. Finally, the samples were reheated to 230 °C at a rate of 10 °C min^{-1}. The registered changes on the calorimetric curves were evaluated.

Fourier transform infrared spectroscopy (FTIR)

Fourier transform infrared spectroscopy (Spectrum 100 PerkinElmer) spectra of samples were recorded using a KBr disk for 40 scans with a resolution of 2 cm^{-1} in the range of 4000 to 400 cm^{-1}.

Hardness and Young's modulus tests

PVP and PVP–CD films were prepared by drying the corresponding solutions on glass slides. A micro-indentation with a Vickers diamond indenter (Fischerscope HM2000, Fischer, Germany) was used to measure the Young's modulus and hardness of the films under 70% RH. Under a load level of 10 mN, the mean values of hardness and Young's modulus were derived from load *vs.* indentation depth curves. At least 5 indentations were performed for each sample.

Scanning electron microscopy (SEM)

SEM images were taken with a Philips, XL30 Environmental scanning electron microscope (ESEM) with a voltage of 10 kV. To have high quality images of polymer microneedle patches, gold coating was applied to the patch.

Microneedle array application to pig skin

The experimental was set according to our previous work.[8] The experiment was performed according to our previously reported work.[8] Pig ears were obtained from the local abattoir and thoroughly cleaned. The ventral side of the ear was lightly shaved and rinsed. The skin was then stored at −20 °C before usage. Before the microneedle array penetration test, the ventral skin (epidermis and dermis) was separated from the cartilage using tweezers and a scalpel. The ventral skin was then stretched on a substrate and four of each type of microneedle array (PVP58 and PVP58–HP-β-CD-11) were applied to the skin with a spring-based applicator. Immediately after the application, the microneedle arrays were removed from the skin. The treated area was excised with biopsy and fixed in 5 ml 4% formaldehyde in 0.1 M phosphate buffered saline overnight. Subsequently, the tissue was washed with 0.1 M phosphate buffered saline. The morphology of the microneedle penetrated pig skin and the used microneedle arrays were observed with ESEM (Philips, XL30).

Results and discussion

FTIR spectra of PVP, CD and PVP–CD complexes

The formation of PVP–CD inclusion complexes was first confirmed by FITR. FTIR is a very useful tool to prove the existence of both guest and host molecules in complexes. Fig. 2a shows the FTIR spectra of PVP58, HP-β-CD, and PVP58–HP-β-CD-11 inclusion complexes. The peak at 3466 cm^{-1} is attributed to the hydroxyl group of water (although the sample was totally dried before FTIR tests), which proves that PVP quickly absorbs water. This peak overlaps with the hydroxyl group of HP-β-CD. The peaks at 3370 cm^{-1}, 2928 cm^{-1}, 1157 cm^{-1}, and 1029 cm^{-1} correspond to the symmetric and antisymmetric stretching of –OH, $–CH_2$ and C–C and the bending vibration of O–H, respectively. The peaks at 2962 cm^{-1}, 2933 cm^{-1}, and 2904 cm^{-1} correspond to the stretching of C–H in the PVP chain.[31]

For HP-β-CD, the peak at 2929 cm^{-1} is the stretching vibration of $–CH_3$ and $–CH_2$. The peaks at 1156 cm^{-1} and 1079 cm^{-1} are the stretching and bending vibrations of C–O–C and C–O–H, respectively. The peaks at 946 cm^{-1} and 856 cm^{-1} correspond to

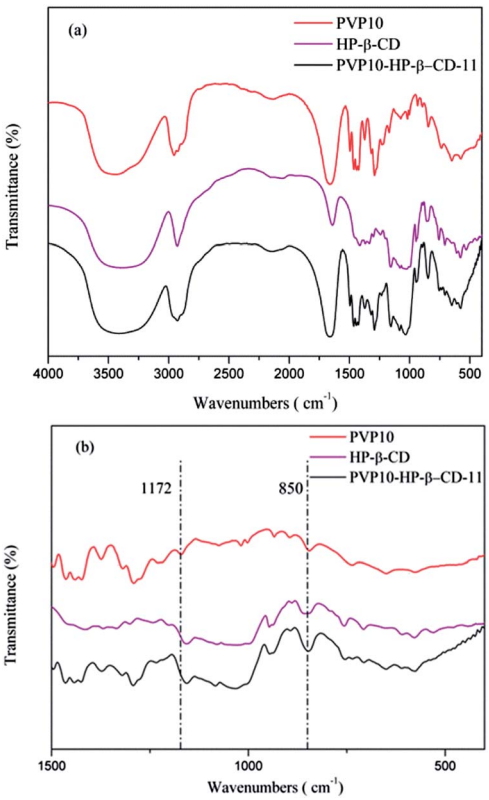

Fig. 2 FTIR spectra of the PVP10, HP-β-CD, and PVP10–HP-β-CD-11 complexes.

α-1,4 skeletal vibrations and a pyranoside bond, respectively. At 757 cm^{-1}, there is a sugar ring breathing vibration peak. The peak at 707 cm^{-1} is a ring vibration peak.

More importantly, the frequency movements of PVP–HP-β-CD inclusion complexes can be seen from Fig. 2b. The axial and angular bending C–C (=O) of PVP is located at 1172 cm^{-1}. After the formation of the complexes, this peak shifts from 16 cm^{-1} to 1156 cm^{-1}. In addition, the peak of the out of plane bending CH_2 of PVP shifts from 850 cm^{-1} to 847 cm^{-1} in the complexes. Overall, the shifts of the two peaks clearly confirm the formation of the PVP–HP-β-CD inclusion complexes. It is caused by the microenvironment change of the CD cavity due to the formation of the inclusion complexes. The increase[32] and decrease[33] of the wavenumbers are dependent on the host–guest interactions. In this work, the non-stoichiometric PVP–CD inclusion complexes are heterogeneous. Parts of *N*-vinylpyrrolidone are included in the β-CD cavity and parts are dangling. The hydrogen bonding between the hydroxyl group of the outer cavity of CD and *N*-vinylpyrrolidone constrains the mobility of the PVP chain, which corresponds to the decrease in the FTIR absorption wavenumbers of stretching and bending vibrations of C–H, C=O and C–N.

Water absorption of PVP and PVP–CD complexes

Water, a plasticizer of amorphous materials, often leads to degradation of their mechanical and thermal properties. Previous FTIR measurements suggested that water molecules

can be bonded to C=O and C–N groups in PVP.[34] A Fourier transform Raman spectrum showed that the change of the properties of PVP *via* water absorption is not only due to hydrogen bonding, but also a result of the plasticizing effect of water.[35] Water molecules distribute uniformly throughout PVP at a concentration of 0.5%, but become remarkably heterogeneous at a higher content.[36] Besides moderately strong hydrogen bonding, extra water molecules are in the free state, which act as plasticizing agents.[37] Therefore, reduction of water absorption by PVP will be beneficial to maintain mechanical and thermal properties. The water absorption of various PVP–CD complexes under different RH conditions is shown in Fig. 3. It can be seen that under different RHs, the water absorption capacity varies. At a low RH of 22%, the water absorption is low. Adding CD to PVP can reduce PVP58 and PVP10 water absorption by only around 1 and 3 wt%, respectively. If we calculate the decrease in water absorption, for PVP10, the water absorption decreases from 8% to 4.9% after 20 days of exposure to the RH 22% environment. This means that the relative decrease of water absorption is about 40%. When the RH increases to 75% and 85%, the effect of CD incorporation is more obvious because a higher RH leads to increased water absorption of PVP. If we compare the water absorption of PVP and PVP–CD inclusion complexes, the following can be observed. The water absorption was 50 wt% and 32 wt% for PVP10 and PVP10–CD complexes, respectively, after 20 days of exposure to the RH 85% environment. This indicates a relative 36% decrease in water absorption. For PVP58, the effect is about the same. At RH 75%, for PVP58, the water absorption drops from 37 wt% to 23% after formation of complexes, which suggests about 38% relative decrease. Overall, the data show that after formation of PVP–CD complexes, water absorption can decrease about 36–40% at different RHs.

Different PVP–CD ratios were investigated in our experiments and the results clearly indicate that the ratio of 1 : 1 worked the best in terms of decreasing water absorption of PVP.

In addition, it can also be found that, at a high RH of 85%, the water absorption of PVP dramatically increases if the time exposure to the environment extends from 10 to 20 days. In comparison, for the PVP–CD complexes, longer time exposure to the environment usually does not lead to increased water absorption. This result suggests that the formation of PVP–CD complexes is good for long term storage.

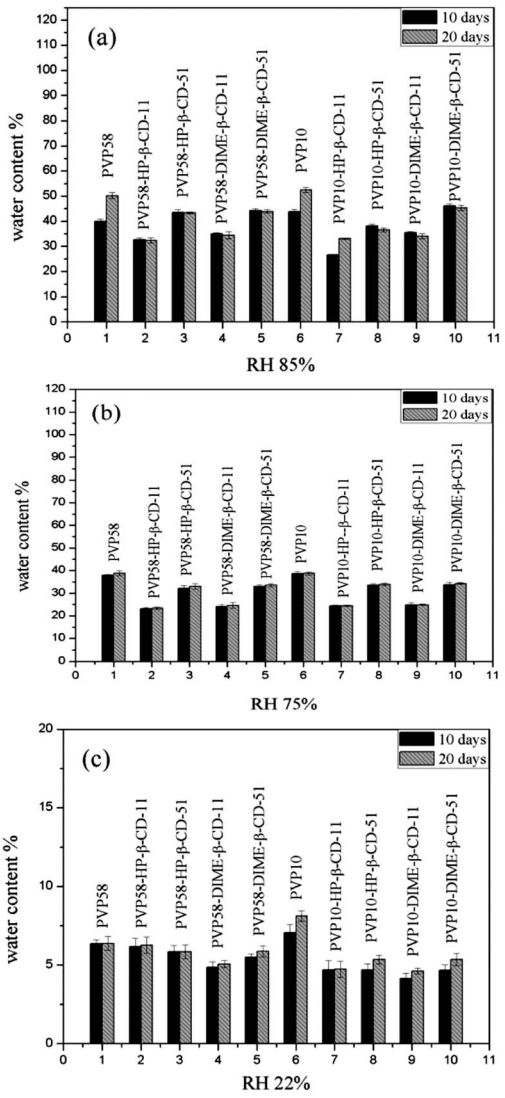

Fig. 3 Water absorption of PVP and PVP–CD complexes under different RHs: (a) RH 85%, (b) RH 75%, and (c) RH 22%.

Glass transition temperatures of PVP and PVP–CD complexes

Fig. 4 presents the DSC curves of PVP58 and PVP58–HP-β-CD-11 inclusion complexes. Compared with PVP, it can be observed that the T_g of PVP58–HP-β-CD-11 is greatly increased from 160 °C to 199 °C, increasing by 39 °C. Table 1 also shows that, after formation of PVP–CD complexes, the glass temperatures increased for various compounds. This is expected because non-stoichiometric polymer–CD inclusion complexes often show different physical properties from the pure one. For example, nylon-6 CD inclusion complexes have higher T_m[38] and non-stoichiometric PMMA–CD inclusion complexes show higher T_g than pure PMMA. In addition, N-s-PCL–α-CD inclusion complexes display shape memory effects depending on the

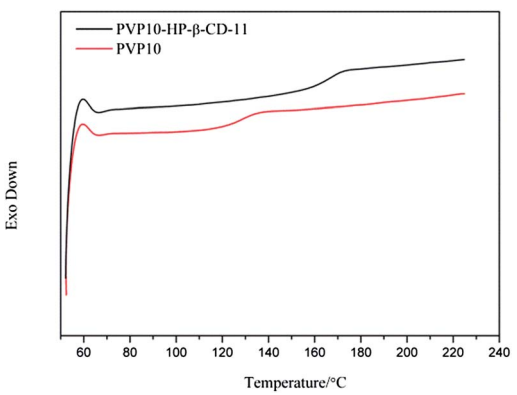

Fig. 4 DSC curves of the PVP and PVP10–HP-β-CD-11 complexes.

Table 1 Glass transition temperatures of PVP and PVP–CD complexes

Sample	T_g (°C)
PVP58	160
PVP58–HP-β-CD-11	199
PVP58–HP-β-CD-51	176
PVP58–DIME-β-CD-11	210
PVP58–DIME-β-CD-51	158
PVP10	128
PVP10–HP-β-CD-11	165
PVP10–HP-β-CD-51	136
PVP10–DIME-β-CD-11	155
PVP10–DIME-β-CD-51	135

coverage of inclusions and the storage modulus is significantly higher than that of the pure PCL.[39]

During glass transition, an amorphous polymer undergoes secondary phase change, changing from a brittle solid state to an elastic rubbery state, reflecting increased chain mobility. As *N*-vinylpyrrolidone is in the inner cavity of CD, the chain mobility is limited and the dangling chain showed a brush structure interacting with the hydroxyl group outside the cavity of CD, both of which contribute to a tighter and more ordered structure.[40]

Mechanical properties of PVP and PVP–CD complexes

The microindentation test results of PVP and PVP–CD complexes are shown in Fig. 5. It can be seen that, after adding CD, the Vickers hardness (HV) and Young's modulus increase. For example, the hardness and Young's modulus of PVP58–HP-β-CD-11 are 127.7 MPa and 2.681 GPa, respectively, which increased by 19.6% and 10.2% in comparison with those of PVP58 with a hardness of 106.8 MPa and Young's modulus of 2.433 GPa, respectively. The hardness and Young's modulus of PVP58–DIME-β-CD-11 showed similar results.

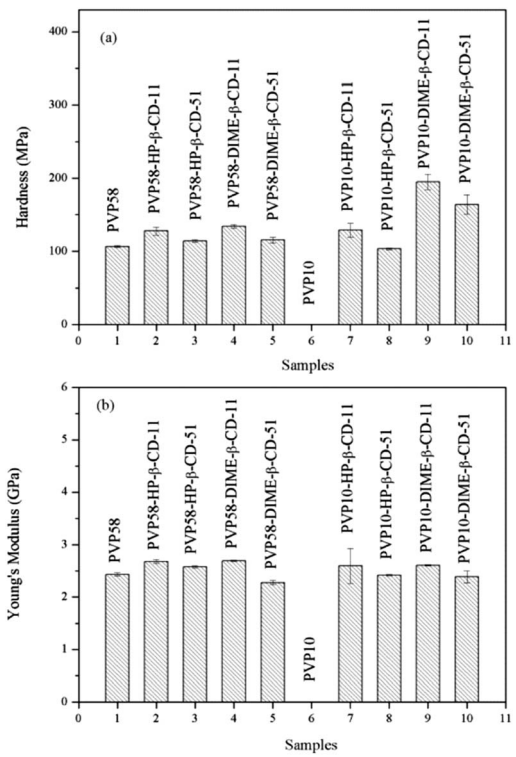

Fig. 5 (a) Hardness and (b) Young's modulus of PVP and PVP–CD complexes.

For PVP10, the strengthening effect is more obvious. The hardness and Young's modulus of PVP10 could not be tested as the samples quickly absorb a high amount of water and became viscous before measurement. In great contrast, after adding CD to PVP10, it can be clearly seen that the hardness and Young's modulus of PVP–CD were close to those of PVP58. For PVP10–HP-β-CD-11 and PVP10–DIME-β-CD-11, the hardness and Young's modulus were 128.7 MPa, 2.598 GPa and 194.8 MPa, 2.611 GPa, respectively. These results proved that the incorporation of CD enhances the mechanical properties, especially for low molecular weight PVP. It is known that low molecular weight PVP has faster water solubility than high molecular weight ones. For microneedles, faster dissolving rates can be very important for vaccine delivery. As indicated by the data, low molecular weight PVP has poor mechanical properties, which restrains its use in this field. Now this problem can be alleviated by adding CD to PVP10 to form complexes. Overall, it can be concluded that the addition of CD significantly increases the mechanical strength of PVP.

If we compare the effect of the ratio of PVP to CD and the type of CD on the mechanical properties of the complexes, it is easy to find that the ratio plays an important role while the type of the tested CD does not have much influence. This is in accordance with previously reported findings[38,39,41] and also in line with the water absorption results. The function of CD has been explained by the schematic diagram in Fig. 1. The CD cavity is occupied by the *N*-vinylpyrrolidone molecules. This host–guest effect constrains the mobility of the polymer chain. Non-stoichiometric CD allows left PVP chains to be still dangling without being encompassed by CD molecules. In this case, the hydrogen bonds formed between left *N*-vinylpyrrolidone and CD molecules will decrease the possibility of water interaction to *N*-vinylpyrrolidone. This is not related to outer space of CD. Therefore, the tested two different CDs had similar effects. However, due to the fact that there are many CD derivatives, this effect of the type of CD on the mechanical properties of the complexes will need further investigation.

Fabrication of PVP and PVP–CD microneedle arrays

Once the properties of PVP and PVP–CD complexes are studied, we next used them to make microneedle arrays and examined their morphology. All microneedle arrays experienced the same manufacturing and processing procedures before scanning electron microscopy observation.

The morphology of microneedles, particularly the radius of the tips, is one of the important factors which may affect the microneedle penetration into the skin.[42] From Fig. 6, it can be found that the morphology of the tips of the PVP and PVP–CD microneedles has great differences. The PVP–CD microneedles

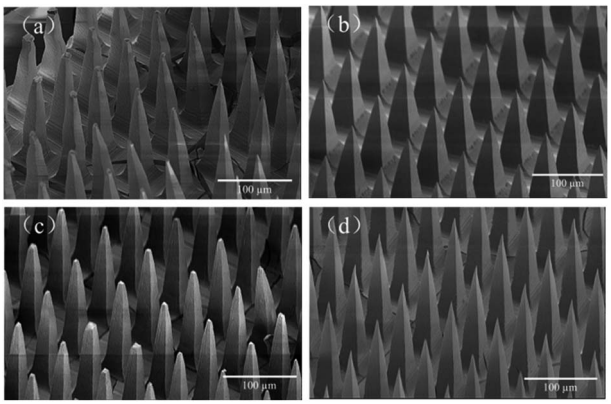

Fig. 6 SEM images of (a) PVP58, (b) PVP58–HP-β-CD-11, (c) PVP10, and (d) PVP10–HP-β-CD-11 microneedle arrays.

have much sharper tips, which allow them to easily penetrate into the skin. And this kind of microneedle has a very low number of cracks on the base. In contrast, many PVP58 microneedle tips are even flat and bent; the base has cracks. This phenomenon is more serious for PVP10 microneedles. The cracks and blunt tips were mainly caused by water absorption.

PVP and PVP–CD microneedle array penetration into the skin

Since the addition of CD to PVP dramatically improved the properties of the microneedle arrays, we further tested the application of the PVP and PVP–CD microneedles to pig skin to find out whether the incorporation of CD can improve the penetration. To perform the test, PVP and PVP–CD microneedle arrays were applied to pig skin separately and the morphology of the treated skin surface and the used microneedle arrays was characterized by ESEM. The SEM images are shown in Fig. 7. From Fig. 7a, it can be seen that the PVP microneedles were not able to pierce the stratum corneum of the pig skin. In great contrast, Fig. 7b clearly shows that the PVP–CD microneedles successfully penetrate into the skin and ordered holes are created due to the penetration of the microneedles into the skin. Because the skin was not completely dehydrated before SEM characterization, the skin would shrink or distort due to water loss during the SEM observation.[43] For PVP microneedle arrays, once applied to the skin, the patches were smashed to many small pieces. Most of the microneedle arrays disappeared after application. For the several remaining microneedles, it was observed that some of them were bent possibly due to the fact that these microneedles were not mechanically strong enough to pierce the stratum corneum of the pig skin (Fig. 7c). In comparison, all of the microneedles of the PVP–CD patches remained after the application. However, the tips of the microneedles were dissolved after being penetrated into the pig skin within a very short period of penetration time (~1 s). Overall, the results clearly indicate that the PVP–CD microneedles can successfully penetrate into the pig skin and rapidly start to dissolve while the pure PVP microneedles with the same manufacturing approach are not capable of piercing the stratum corneum of the skin.

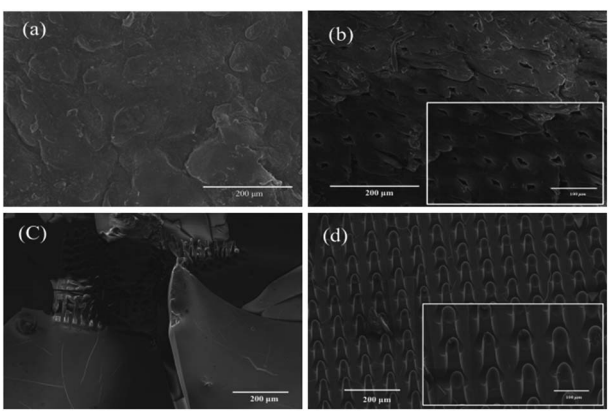

Fig. 7 SEM images of (a) pig skin after PVP58 microneedle array application; (b) pig skin after PVP58–HP-β-CD-11 microneedle array application; (c) PVP58 microneedle arrays after pig skin application tests; (d) PVP58–HP-β-CD-11 microneedle arrays after pig skin application tests.

Conclusions

In conclusion, PVP–CD inclusion complexes were successfully prepared. The influence of PVP to CD ratios and CD species on the mechanical properties, thermal properties and water absorption of different molecular weight PVP was studied. With the addition of CD, the water absorption of the PVP–CD complexes reduced as much as 36–40% in comparison with that of PVP. Meanwhile, the mechanical properties and T_g of the complexes were also increased. With the improved properties, the PVP–CD microneedles possess very sharp tips and the patches contain a low number of cracks. Pig skin application results suggested that the PVP–CD microneedle arrays were able to reliably pierce the stratum corneum of the skin while it was not achievable for the PVP microneedles with the same manufacturing approach. We expect that the PVP–CD microneedle arrays are more suitable for vaccine delivery.

Acknowledgements

This study was funded by the City University of Hong Kong (Project no. 7200247 and 9667068).

Notes and references

1 M. R. Prausnitz and R. Langer, *Nat. Biotechnol.*, 2008, **26**, 1261–1268.
2 T. Tanner and R. Marks, *Skin Res. Technol.*, 2008, **14**, 249–260.
3 K. van der Maaden, W. Jiskoot and J. Bouwstra, *J. Controlled Release*, 2012, **161**, 645–655.
4 R. H. E. Chong, E. Gonzalez-Gonzalez, M. F. Lara, T. J. Speaker, C. H. Contag, R. L. Kaspar, S. A. Coulman, R. Hargest and J. C. Birchall, *J. Controlled Release*, 2013, **166**, 211–219.

5 S. Bhattacharya, D. H. Kam, L. J. Song and J. Mazumder, *Metall. Mater. Trans. A*, 2012, **43**, 2574–2580.
6 M. L. Crichton, B. C. Donose, X. Chen, A. P. Raphael, H. Huang and M. A. F. Kendall, *Biomaterials*, 2011, **32**, 4670–4681.
7 C. O'Mahony, A. Blake, J. Scully, J. O'Brien and A. C. Moore, *J. Pharm. Pharmacol.*, 2010, **62**, 799.
8 L. Yan, A. P. Raphael, X. Zhu, B. Wang, W. Chen, T. Tang, Y. Deng, H. J. Sant, G. Zhu, K. W. Choy, B. K. Gale, T. W. Prow and X. Chen, *Adv. Healthcare Mater.*, DOI: 10.1002/adhm.201300312.
9 P. C. DeMuth, W. F. Garcia-Beltran, M. L. Ai-Ling, P. T. Hammond and D. J. Irvine, *Adv. Funct. Mater.*, 2013, **23**, 161–172.
10 M. C. Chen, M. H. Ling, K. Y. Lai and E. Pramudityo, *Biomacromolecules*, 2012, **13**, 4022–4031.
11 M. C. Chen, S. F. Huang, K. Y. Lai and M. H. Ling, *Biomaterials*, 2013, **34**, 3077–3086.
12 J. W. Lee, J.-H. Park and M. R. Prausnitz, *Biomaterials*, 2008, **29**, 2113–2124.
13 S. P. Sullivan, N. Murthy and M. R. Prausnitz, *Adv. Mater.*, 2008, **20**, 933–938.
14 K. Tsioris, W. K. Raja, E. M. Pritchard, B. Panilaitis, D. L. Kaplan and F. G. Omenetto, *Adv. Funct. Mater.*, 2012, **22**, 330–335.
15 C. J. Martin, C. J. Allender, K. R. Brain, A. Morrissey and J. C. Birchall, *J. Controlled Release*, 2012, **158**, 93–101.
16 N. Roy, N. Saha, T. Kitano and P. Saha, *J. Appl. Polym. Sci.*, 2010, **117**, 1703–1710.
17 S. A. Papadimitriou, P. Barmpalexis, E. Karavas and D. N. Bikiaris, *Eur. J. Pharm. Biopharm.*, 2012, **82**, 175–186.
18 J. Zhang and P. X. Ma, *Adv. Drug Delivery Rev.*, 2013, **65**, 1215–1233.
19 E. M. M. D. Valle, *Process Biochem.*, 2004, **39**, 1033–1046.
20 Y. Yang, Y. Chen and Y. Liu, *Inorg. Chem.*, 2006, **45**, 3014–3022.
21 Y. Liu, Y. W. Yang, Y. Chen and F. Ding, *Bioorg. Med. Chem.*, 2005, **13**, 963–971.
22 Y. Liu, Y. Yang, Y. Song, H. Y. Zhang, F. Ding, T. Wada and Y. Inoue, *ChemBioChem*, 2004, **5**, 868–871.
23 Y. Liu, Y. Yang, E. Yang and X. Guan, *J. Org. Chem.*, 2004, **69**, 6590–6602.
24 K. Uekama, F. Hirayama and H. Arima, *J. Inclusion Phenom. Macrocyclic Chem.*, 2006, **56**, 3–8.
25 J. Wang, J. Y. Zong, D. Zhao, R. X. Zhuo and S. X. Cheng, *Colloids Surf., B*, 2011, **87**, 198–202.
26 W. Song, X. W. Yu, S. X. Wang, R. Blasier, D. C. Markel, G. Z. Mao, T. Shi and W. P. Ren, *Int. J. Nanomed.*, 2011, **6**, 3173–3186.
27 V. A. Marcolino, G. M. Zanin, L. R. Durrant, M. D. Benassi and G. Matioli, *J. Agric. Food Chem.*, 2011, **59**, 3348–3357.
28 Y.-L. Wu, H. Yin, F. Zhao and J. Li, *Adv. Healthcare Mater.*, 2013, **2**, 297–301.
29 P. C. DeMuth, W. F. Garcia-Beltran, M. L. Ai-Ling, P. T. Hammond and D. J. Irvine, *Adv. Funct. Mater.*, 2013, **23**, 161–172.
30 J. Teng, S. Bates, D. A. Engers, K. Leach, P. Schields and Y. L. Yang, *J. Pham. Sci.*, 2010, **99**, 3815–3825.
31 L.-S. Wan, X.-J. Huang and Z.-K. Xu, *J. Phys. Chem. B*, 2007, **111**, 922–928.
32 B. Williamson and A. Tonelli, *J. Inclusion Phenom. Macrocyclic Chem.*, 2012, **72**, 71–78.
33 L. C. Mendes, R. C. Rodrigues and E. P. Silva, *J. Therm. Anal. Calorim.*, 2010, **101**, 899–905.
34 H. Luo, Y. Liu, Z. Yu, S. Zhang and B. Li, *Biomacromolecules*, 2008, **9**, 2573–2577.
35 T. Uyar, C. C. Rusa, M. A. Hunt, E. Aslan, J. Hacaloglu and A. E. Tonelli, *Polymer*, 2005, **46**, 4762–4775.
36 W. G. Rothschild, *J. Am. Chem. Soc.*, 1972, **94**, 8676–8683.
37 L. S. Taylor, F. W. Langkilde and G. Zografi, *J. Pham. Sci.*, 2001, **90**, 888–901.
38 E. Kaya and L. J. Mathias, *J. Polym. Sci., Part A: Polym. Chem.*, 2010, **48**, 581–592.
39 H. Hamdi, R. Abderrahim and F. Meganem, *Spectrochim. Acta, Part A*, 2010, **75**, 32–36.
40 A. Mohan, X. Joyner, R. Kotek and A. E. Tonelli, *Macromolecules*, 2009, **42**, 8983–8991.
41 T.-X. Xiang and B. Anderson, *Pharm. Res.*, 2005, **22**, 1205–1214.
42 S. P. Davis, B. J. Landis, Z. H. Adams, M. G. Allen and M. R. Prausnitz, *J. Biomech.*, 2004, **37**, 1155–1163.
43 A. Boyde and E. Maconnachie, *Scanning Electron Microsc.*, 1981, **4**, 27–34.